



## Hypothetical three-dimensional all- $sp^2$ carbon phase

G.-M. Rignanese and J.-C. Charlier

*Unité de Physico-Chimie et de Physique des Matériaux (PCPM), European Theoretical Spectroscopy Facility (ETSF), Université catholique de Louvain, Place Croix du Sud 1, 1348 Louvain-la Neuve, Belgium*

(Received 28 April 2008; published 17 September 2008)

The structural and the electronic properties of a hypothetical three-dimensional (3D) all- $sp^2$  carbon phase, called  $K_4$ , are investigated using first-principles calculations. The cohesive energy per atom for this structure is found to be 1.3 eV lower than for graphite and diamond, but also more than 0.3 eV lower than for the previously proposed H-6, bct-4, and C-20 phases, also 3D all- $sp^2$  carbon forms. The calculated bulk modulus for the  $K_4$  crystal is slightly higher than for the C-20 structure but lower than for the H-6 and bct-4 solids. Our analysis reveals that the relatively low cohesive energy and bulk modulus of the  $K_4$  phase are due to the disruption of the  $\pi$  bonding states. The calculated density of states and band structure show that the  $K_4$  phase is metallic.

DOI: [10.1103/PhysRevB.78.125415](https://doi.org/10.1103/PhysRevB.78.125415)

PACS number(s): 61.50.Ah, 62.20.de, 64.60.My, 71.15.Mb

Unquestionably, carbon is the most versatile element of the periodic table. The organics, the largest group of compounds, owe their existence to its ability to simultaneously bond to itself and a variety of heteroatoms. Moreover, pure carbon allotropes offer a unique richness and diversity: from the recently synthesized single sheet of grapheme<sup>1</sup> to the fullerenes<sup>2</sup> or the nanotubes.<sup>3</sup>

In the quest of new hard or low compressibility materials, pure carbon allotropes have also attracted considerable attention based on the belief that the bond length and strength are related (the shorter the bonds, the stronger). Indeed, in the well-known pure carbon allotropes, the bond length strongly depends on the hybridization: from  $\sim 1.42$  Å for graphite ( $sp^2$ ) to  $\sim 1.54$  Å for diamond ( $sp^3$ ). However, despite its shorter bond length graphite is known as an excellent lubricant, and diamond, in contrast, is known as the hardest material. The problem is that graphite is intrinsically soft because of its two-dimensional (2D) nature. Hence, several hypothetical three-dimensional (3D) all- $sp^2$  networks have been proposed in the literature<sup>4</sup> such as H-6,<sup>5</sup> bct-4,<sup>6</sup> and C-20<sup>7</sup> structures (see Fig. 1), all of them revealing high bulk moduli but unfortunately smaller than the value for diamond.

Recently, Sunada<sup>8</sup> proposed to use the structural principles of the diamond lattice to create a related crystal, called  $K_4$ , with equal mathematical symmetry, inducing isotropic properties. In this topology, the atoms are not tetragonally but trigonally bonded, thus constituting a hypothetical 3D all- $sp^2$  network (see Fig. 1). Since “*Nature favors symmetry*,” one is tempted to ask if this high-symmetry mathematical object can exist in nature as a real crystal or if it may be synthesized with a highly versatile atomic element like carbon.

In this paper, this hypothetical 3D all- $sp^2 K_4$  carbon allotropic form is investigated using first-principles calculations. Its structural and electronic properties are determined and compared to those of all the other carbon phases illustrated in Fig. 1. The cohesive energy per atom for the  $K_4$  structure is more than 0.3 eV lower than for all the 3D all- $sp^2$  carbon forms proposed previously (H-6, bct-4, and C-20). The bulk modulus for the  $K_4$  crystal is slightly higher than for the C-20 structure but lower than for the H-6 and bct-4 solids.

The relatively low cohesive energy and bulk modulus of this phase are discussed in terms of the disruption of the  $\pi$  bonding states. The  $K_4$  phase is also found to be metallic. Our findings question the possibility to create carbon materials harder than diamond using 3D structure out of a  $sp^2$ -bonded atomic configuration.

Throughout this study, the structural and electronic properties of the different allotropic carbon phases are investigated within a pseudopotential<sup>9</sup> plane-wave approach to density functional theory (DFT), as implemented in the ABINIT code.<sup>10</sup> We adopt the local density approximation (LDA) and a 30 Ha cutoff to expand the electronic eigenstates. Special care is taken to sample the Brillouin zone of metallic carbon phases using various sets of irreducible k points.<sup>11</sup> The en-

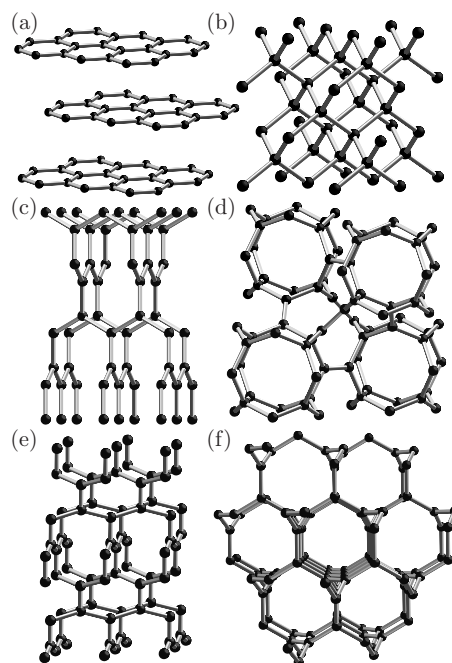


FIG. 1. Ball and stick models of the two natural carbon forms: (a) graphite and (b) diamond compared to four hypothetical 3D all- $sp^2$  carbon phases: (c) H-6, (d) C-20, (e) bct-4, and (f)  $K_4$  crystals.

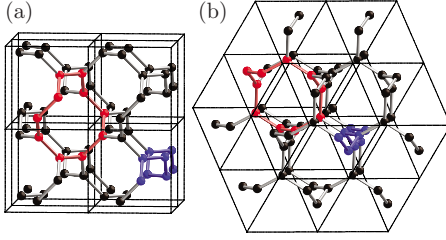


FIG. 2. (Color online)  $K_4$  structure viewed from the (a)  $[1\ 0\ 0]$  and (b)  $[1\ 1\ 1]$  directions. The 8 atom unit cell is repeated twice in each direction. The chiral property of the crystal is illustrated by highlighting (a) the spiraling squares (blue) connected to octagons and (b) the spiraling triangles (blue) connected to nonagons. In both cases, the decagonal rings (see text) are represented in red.

ergy levels are populated using a Gaussian broadening<sup>12</sup> of 150 meV. The structural parameters are relaxed using a Broyden scheme for the forces and stresses, to values lower than  $10^{-6}$  Ha/Bohr and  $10^{-6}$  Ha/Bohr<sup>3</sup>, respectively.

The hypothetical  $K_4$  structure is body-centered cubic (space group  $I4_122$ ), with eight atoms located at the  $8a$  ( $1/8, 1/8, 1/8$ ) Wyckoff positions in the conventional unit cell (the primitive unit cell only contains four atoms). Different views of the structure are presented in Fig. 2. This crystal has been created by similarity to that of diamond using mathematical considerations.<sup>8</sup> Both have a very high symmetry which results in a unique type of bond ( $sp^2$  for the  $K_4$  structure and  $sp^3$  for diamond). But, while the 3D diamond lattice presents hexagonal rings in projection, the  $K_4$  space-filling structure shows decagonal rings in projection, colored in red in Fig. 2. In addition, a significant difference between the  $K_4$  structure and the diamond crystal is the presence of *chirality*. Namely, its mirror image cannot be superposed on the original one by a rigid motion, like for DNA, chemical enantiomers, ( $n, m \neq n \neq 0$ ) nanotubes, ... The chirality of the  $K_4$  structure can be seen from the spiraling square-octagon and triangle-nonagon polygons, highlighted in blue in Figs. 2(a) and 2(b), respectively.

The structural properties of all the carbon phases illustrated in Fig. 1 (namely, graphite, diamond, bct-4, H-6, C-20,

and  $K_4$ ) are summarized in Table I. For each form, we calculate the total energy over a wide range of volumes. At a given volume, the atomic positions and the unit cell are fully relaxed. We fit the resulting energies to a Birch equation of state to calculate the bulk moduli. The cohesive energy is determined by subtracting the total energy of an isolated carbon atom.

In contrast with the other 3D all- $sp^2$  crystals, there is only one C-C bond length in the  $K_4$  structure (due to its high symmetry). It is calculated to be very close to that found in most  $sp^2$  systems both in 2D, graphite (1.42 Å) or  $C_{60}$  (1.40 Å, 1.45 Å), and in 3D all- $sp^2$  crystals, H-6 and bct-4. In the C-20 structure, however, a shorter bond length (1.34 Å) also appears (in agreement with Ref. 7), which is associated with a double bond. Such an alternation of single (longer) and double (shorter) bonds is quite frequent in carbon systems (e.g., the  $C_{60}$  molecule). However, it is excluded by symmetry in the  $K_4$  crystal.

Calculations based on the local-density approximation tend to overestimate the cohesive energy of solids but the relative energies of different atomic structures are usually reliable. The cohesive energy of the  $K_4$  solid is found to be 8.9 eV per atom (Table I), which is  $\sim 1.3$  eV lower than the binding energy of graphite and also  $\sim 0.9$  eV lower than the one of  $C_{60}$  (Ref. 13) within this technique. Such a low stability of the  $K_4$  crystal compared to the other all- $sp^2$  forms will be explained in the following sections using a topological model based on the disruption of the  $\pi$  bonding.

Concerning the bulk modulus, the compressibility of the  $K_4$  solid is predicted to be higher compared to diamond and to two other 3D all- $sp^2$  carbon solids (H-6, bct-4), but slightly lower than the C-20 solid phase. In Table I, a correlation can be observed between the bulk modulus and the inverse of the volume per atom (rather than the inverse of the C-C bond length as usually thought). In fact, the large volume per atom predicted for the  $K_4$  structure is certainly responsible for such a surprisingly compressible carbon structure, as also observed for most cagelike materials such as the C-20 solid,<sup>7</sup> carbon clathrates,<sup>14</sup> and carbon foams.<sup>15,16</sup>

The electronic band structure of the  $K_4$  solid and the cor-

TABLE I. Equilibrium structural parameters (space group, atomic positions, volume  $V$ , lattice parameters  $a$  and  $c$ , bond lengths  $d_{C-C}$ ), cohesive energy  $E_{\text{coh}}$ , and bulk modulus  $B$  calculated for the  $K_4$  carbon solid and for H-6, bct-4, C-20, graphite and diamond. For the anisotropic structures (H-6, bct-4, and graphite), the isotropic value of the bulk modulus is also indicated between parentheses.

	$K_4$	H-6	bct-4	C-20	Graphite	Diamond
Space group	$I4_132$	$P6_222$	$I4_1/amd$	$Fm\bar{3}m$	$P6_3/mmc$	$Fd\bar{3}m$
Atomic positions	$8a$ $(\frac{1}{8}, \frac{1}{8}, \frac{1}{8})$	$6e$ $(x, x, x)$ $x=0.1090$	$8e$ $(0, 0, z)$ $z=0.0860$	$32f; 48h$ $(x, x, x); (0, y, y)$ $x=0.1391; y=0.1976$	$2b; 2c$ $(0, 0, \frac{1}{4}); (\frac{1}{3}, \frac{2}{3}, \frac{1}{4})$	$8a$ $(\frac{1}{8}, \frac{1}{8}, \frac{1}{8})$
$V(\text{\AA}^3/\text{atom})$	8.39	6.15	6.67	9.13	8.45	5.44
$a(\text{\AA})$	4.063	2.604	2.500	9.007	2.434	3.518
$c(\text{\AA})$		6.283	8.531		6.596	
$d_{C-C}(\text{\AA})$	1.437	1.434, 1.460	1.416, 1.467	1.336, 1.457	1.405	1.523
$E_{\text{coh}}$ (eV)	8.903	9.373	9.682	9.247	10.206	10.203
$B$ (GPa)	273	384 (399)	354 (369)	247	29 (293)	466

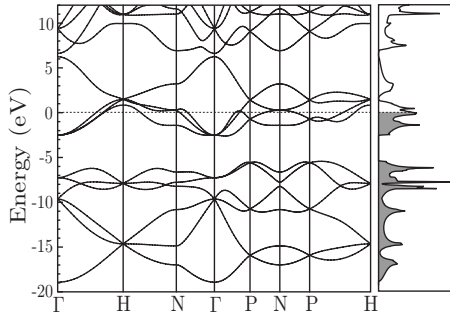


FIG. 3. Electronic band structure (left) along different high-symmetry lines and the corresponding density of states (right) for the  $K_4$  solid. The Fermi energy is positioned at zero.

responding density of states are reported in Fig. 3, showing a metallic behavior. These can be interpreted using the procedure of Ref. 17 to generate maximally localized Wannier functions. Usually, in all- $sp^2$  configurations, one  $2s$  and two  $2p$  atomic orbitals of each carbon atom undergo hybridization to form three  $sp^2$  orbitals that have a trigonal planar geometry. These hybridized orbitals overlap with those of the three neighboring carbon atoms to form three  $\sigma$  (bonding) and three  $\sigma^*$  (antibonding) orbitals (per pair of carbon atoms). In the  $K_4$  structure, we find six such  $\sigma$  orbitals, as illustrated in Fig. 4(a), for the manifold ranging from  $-20$  to  $-5$  eV. Higher in energy, the states localized between  $-3$  and  $6$  eV correspond to the four (one per carbon atom) remaining  $2p_z$  orbitals (where  $z$  is the direction perpendicular to the plane formed by the atom and its first neighbors), as represented in Fig. 4(b). This separation between the lower energy  $\sigma$  states and the higher energy  $2p_z$  states of carbon is also present in other all- $sp^2$  carbon materials such as graphene<sup>18</sup> and graphite.<sup>19</sup>

The  $2p_z$  orbital of each carbon atom overlaps with those of its first neighbors to create the delocalized  $\pi$  (bonding) and  $\pi^*$  (antibonding) orbitals. However, the amount of overlap depends on the angle between the  $2p_z$  orbitals of the neighboring carbon atoms (also called misalignment angle  $\phi$  in Haddon's theory<sup>20,21</sup>). When the angle increases, the  $\pi$  bonding between these atoms—and thus the binding energy of the solid—decreases. In graphene, all the  $2p_z$  orbitals are aligned with the direction perpendicular to the sheet,<sup>22</sup> leading to a strong  $\pi$  bonding interaction between carbon neighbors, and thus contributing to the high stability of the system. In contrast, in the  $K_4$  solid, the  $2p_z$  orbitals between neigh-

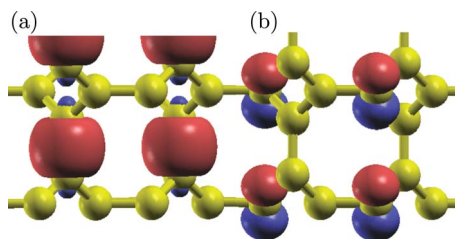


FIG. 4. (Color online) Isosurface of (a) a  $\sigma$  and (b) a  $2p_z$  Wannier function in the  $K_4$  crystalline structure (yellow). The positive and negative lobes of the localized atomic orbitals, are illustrated in blue and red, respectively.

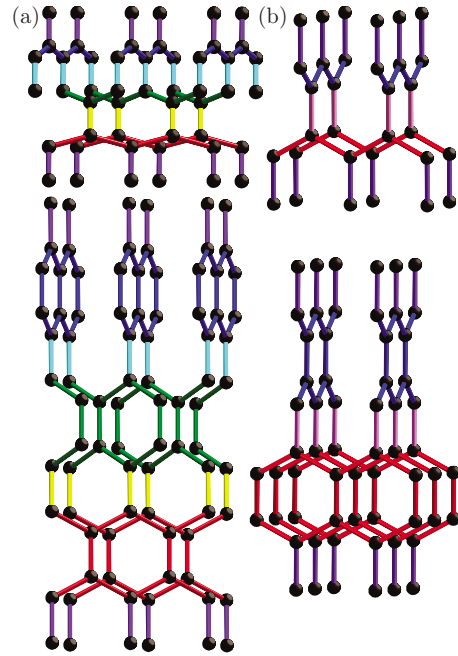


FIG. 5. (Color online) Ball and stick models of the (a) H-6 and (b) bct-4 crystals (top) and their corresponding extended structures (bottom). The bonds with well-aligned  $2p_z$  orbitals are colored in pink, violet, turquoise, and yellow.

oring atoms are all strongly misaligned, leading to a disruption of the  $\pi$  bonding network and to a metastability of this phase. This effect of disrupting the  $\pi$  bonding state has already been observed in fullerenes<sup>23</sup> and in the three other 3D all- $sp^2$  solids.<sup>5-7</sup>

In fact, the local environment of each atom influences its ability to form these  $\pi$  bonds with its neighbors and hence the stability of the crystal. The differences in cohesive energy for 3D all- $sp^2$  solids reflect the amount of misaligned  $2p_z$  orbitals in the structure. Graphite has all its  $2p_z$  orbitals perfectly aligned and is the most stable crystal. Conversely, all the  $2p_z$  orbitals are all misaligned in the  $K_4$  solid which is the most unstable. The C-20 structure, which presents only 1/5 of its bonds with well-aligned  $2p_z$  orbitals, is less stable than the H-6 and bct-4 ones, which both have 2/3 of their bonds with well-aligned  $2p_z$  orbitals. These two solids only differ by the value of the misalignment angles ( $\phi=60^\circ$  in H-6 and  $\phi=90^\circ$  in bct-4); it is thus more dubious to compare their stability using such a qualitative model.

In order to further investigate these topological considerations, other 3D all- $sp^2$  structures containing more bonds with well-aligned  $2p_z$  orbitals were generated based on the H-6 and bct-4 solids, since for symmetry reasons this could not be done based on the  $K_4$  crystal. As shown in Fig. 5(a), the H-6 structure can be seen as consisting of three families of limited-dimension graphene planes (colored in red, green, and blue) with well-aligned  $2p_z$  orbitals, connected by bonds (in violet, yellow, and turquoise) with misaligned  $2p_z$  orbitals with  $\phi=60^\circ$  (it is actually the angle from one plane to another). As reported in Fig. 5(b), the bct-4 crystal only has two such families of planes (in red and blue) and the connecting bonds (in pink and violet) present a misalignment of  $90^\circ$ . For both systems, the number of bonds with well-

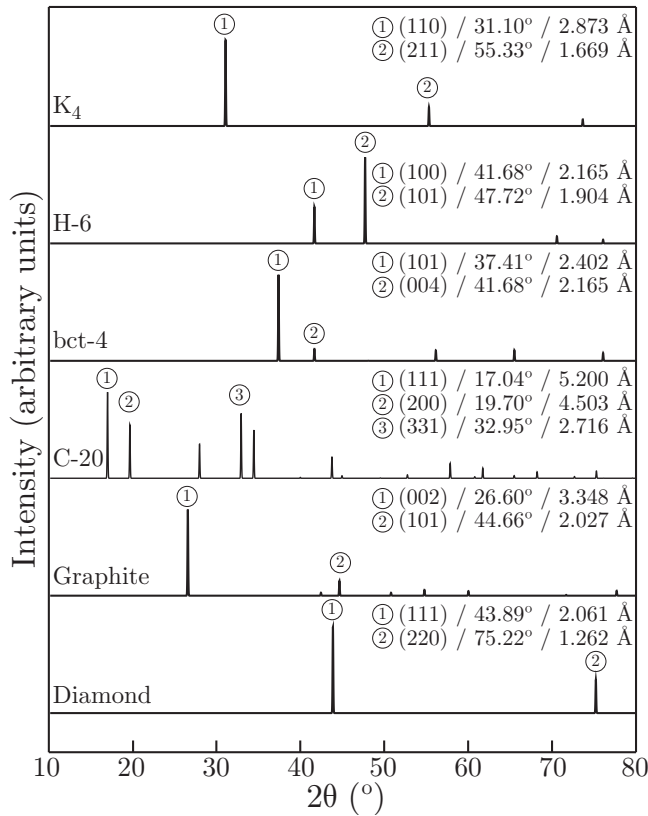


FIG. 6. X-Ray diffraction patterns simulated (Ref. 27) for the different carbon structures considered in the present study. The Miller indices, the precise value of  $2\theta$ , and the corresponding interplane distance are reported for the most prominent peaks of each structure.

aligned  $2p_z$  orbitals can easily be increased by extending the dimension of the families of graphene planes to form hypergraphite as suggested in Refs. 24–26. This is illustrated at the bottom of Fig. 5. The amount of such bonds goes from 2/3 to 5/6 when going from the H-6 and bct-4 crystals to their corresponding extended structures. The cohesive energy of the extended systems are found to be increased by  $\approx 0.1$  eV/atom with respect to the original ones, confirming the trend already observed for the other all- $sp^2$  solids.

In contrast, the bulk moduli of the extended structures 384 and 350 GPa are basically the same as for the H-6 and bct-4 crystals, respectively. This indicates that increasing the number of bonds with well-aligned  $2p_z$  orbitals is probably not the route to follow to obtain a 3D all- $sp^2$  material harder than diamond. On the other hand, not only the bulk moduli but also the volume per atom are not changed in the extended structures. This further confirms our observation that the

bulk modulus correlates with the inverse of the volume per atom. This suggests that trying to reduce the volume per atom might be a more appropriate solution. But this is not possible for 3D all- $sp^2$  materials. Thus, it seems unavoidable to us that such systems will present a bulk modulus lower than diamond.

In conclusion, a hypothetical 3D all- $sp^2$  crystal, named  $K_4$ , having a remarkable symmetric and isotropic structure mathematically similar to that of diamond, has been investigated using first-principles approach. The equilibrium geometry (internal and lattice parameters), the cohesive energy, and the bulk moduli were calculated and compared to those of other 3D all- $sp^2$  crystals. The carbon-carbon bond length is close to graphite and to other 3D all- $sp^2$  systems such as H-6 and bct-4. Due to the symmetry of the  $K_4$  solid, all the bonds are equivalent so that alternation of single and double bonds like in the C-20 crystal is not possible. The cohesive energy per atom for the  $K_4$  structure is quite low: it is significantly lower than that of all the 3D all- $sp^2$  carbon forms proposed previously (H-6, bct-4, and C-20). This low cohesive energy has been explained by the misalignment of the  $2p_z$  orbitals in all the bonds. The bulk modulus for the  $K_4$  crystal is found to be lower than for the H-6 and bct-4 solids, but slightly higher than for the C-20 structure. The electronic properties (band structure and density of states) have also been calculated. The  $K_4$  phase is found to be metallic, with the partially occupied manifold close to the Fermi energy corresponding to the four  $2p_z$  orbitals.

Even though the  $K_4$  structure is found to be metastable for carbon, it is an interesting example of a 3D all- $sp^2$  network. Its x-ray signature should be easily identifiable experimentally with respect to the other carbon structures, as shown in Fig. 6. If the  $K_4$  solid was to be synthesized, it certainly would have interesting material properties. For instance, assuming an electron-phonon coupling analogous to graphite ( $\pm$  same C-C bond length) and its intrinsic metallic behavior, the  $K_4$  solid might be an interesting superconducting material.

#### ACKNOWLEDGMENTS

G.M.R. and J.C.C. acknowledge the FNRS of Belgium for financial support. Parts of this work are directly connected to the Belgian Program on Interuniversity Attraction Poles (PAI6) on “Quantum Effects in Clusters and Nanowires,” to the ARC sponsored by the Communauté Française de Belgique, and to the NANOQUANTA European Network of Excellence. Computational resources have been provided by the Université catholique de Louvain; all the numerical simulations have been performed on the LEMAITRE computer of the CISM.

<sup>1</sup>K. S. Novoselov, A. K. Geim, S. V. Morozov, D. Jiang, S. V. Dubonos, I. V. Girgorieva, and A. A. Firsov, *Science* **306**, 666 (2004).

<sup>2</sup>H. W. Kroto, J. R. Heath, S. C. O’Brien, R. F. Curl, and R. E. Smalley, *Nature (London)* **318**, 162 (1985).

<sup>3</sup>S. Iijima, *Nature (London)* **354**, 56 (1991).

<sup>4</sup>R. Hoffmann, T. Hughbanks, M. Kertesz, and P. H. Bird, *J. Am. Chem. Soc.* **105**, 4831 (1983).

<sup>5</sup>A. Y. Liu, M. L. Cohen, K. C. Hass, and M. A. Tamar, *Phys. Rev. B* **43**, 6742 (1991).

- <sup>6</sup>A. Y. Liu and M. L. Cohen, Phys. Rev. B **45**, 4579 (1992).
- <sup>7</sup>M. Côté, J. C. Grossman, M. L. Cohen, and S. G. Louie, Phys. Rev. B **58**, 664 (1998).
- <sup>8</sup>T. Sunada, Not. Am. Math. Soc. **55**, 208 (2008).
- <sup>9</sup>N. Troullier and J. L. Martins, Phys. Rev. B **43**, 1993 (1991).
- <sup>10</sup>X. Gonze *et al.*, Comput. Mater. Sci. **25**, 478 (2002).
- <sup>11</sup>H. J. Monkhorst and J. D. Pack, Phys. Rev. B **13**, 5188 (1976).
- <sup>12</sup>M. Methfessel and A. T. Paxton, Phys. Rev. B **40**, 3616 (1989).
- <sup>13</sup>X. Rocquefelte, G.-M. Rignanese, V. Meunier, H. Terrones, M. Terrones, and J.-C. Charlier, Nano Lett. **4**, 805 (2004).
- <sup>14</sup>X. Blase, P. Gillet, A. San Miguel, and P. Mélinon, Phys. Rev. Lett. **92**, 215505 (2004).
- <sup>15</sup>K. Umemoto, S. Saito, S. Berber, and D. Tománek, Phys. Rev. B **64**, 193409 (2001).
- <sup>16</sup>A. Kuc and G. Seifert, Phys. Rev. B **74**, 214104 (2006).
- <sup>17</sup>N. Marzari and D. Vanderbilt, Phys. Rev. B **56**, 12847 (1997).
- <sup>18</sup>J.-C. Charlier, P. C. Eklund, J. Zhu, and A. C. Ferrari, in *Carbon Nanotubes*, edited by A. Jorio, G. Dresselhaus, and M. S. Dresselhaus (Springer-Verlag, Berlin, 2008); Top. Appl. Phys. **111**, 673709 (2008).
- <sup>19</sup>J.-C. Charlier, X. Gonze, and J.-P. Michenaud, Phys. Rev. B **43**, 4579 (1991).
- <sup>20</sup>R. C. Haddon, Chem. Phys. Lett. **125**, 231 (1986).
- <sup>21</sup>R. C. Haddon, J. Am. Chem. Soc. **108**, 2837 (1986).
- <sup>22</sup>P. R. Wallace, Phys. Rev. **71**, 622 (1947).
- <sup>23</sup>J. C. Grossman, M. Côté, S. G. Louie, and M. L. Cohen, Chem. Phys. Lett. **284**, 344 (1998).
- <sup>24</sup>Y. Takagi, M. Fujita, M. Igami, K. Kusakabe, K. Wakabayashi, and K. Nakada, Synth. Met. **103**, 2574 (1999).
- <sup>25</sup>Y. Takagi, M. Fujita, and K. Kusakabe, Mol. Cryst. Liq. Cryst. **340**, 379 (2000).
- <sup>26</sup>Y. Takagi, M. Fujita, K. Wakabayashi, M. Igami, S. Okada, K. Nakada, and K. Kusakabe, arXiv:cond-mat/0001027 (unpublished).
- <sup>27</sup>D. C. Palmer, *Computer Program CrystalDiffract 5.1.6* (Crystal-Maker Software, Bicester, 2008).